Joint Received Signal Strength, Angle-of-Arrival, and Time-of-Flight Positioning

David Plets[1], Wouter Deprez, Jens Trogh[1], Luc Martens[1], Wout Joseph[1]
[1]imec-WAVES, Dept. of Information Technology, Ghent University, Ghent, Belgium
david.plets@ugent.be

***Abstract*—This paper presents a software positioning framework that is able to jointly use measured values of three parameters: the received signal strength, the angle-of-arrival, and the time-of-flight of the wireless signals. Based on experimentally determined measurement accuracies of these three parameters, results of a realistic simulation scenario are presented. It is shown that for the given configuration, angle-of-arrival and received signal strength measurements benefit from a hybrid system that combines both. Thanks to their higher accuracy, time-of-flight systems perform significantly better, and obtain less added value from a combination with the other two parameters.**

***Index Terms*—positioning, algorithm, AoA, ToF, ToA, RSS, RSSI, location, tracking, localization, indoor, metric, simulation, model, modeling, Angle-of-Arrival, Time-of-Flight, Time-of-Arrival, Received Signal Strength, Received Signal Strength Indicator.**

I. Introduction

Indoor positioning and tracking has gained a lot of research attention in recent years, thanks to the many applications, in e.g., hospitals, malls, airports, train stations, industrial warehouses, musea, office buildings. Localization and navigation solutions are being installed for the purpose of efficiency, safety, advertising, comfort,... Different approaches are currently being researched, where the trade-off between location accuracy and installation and deployment cost is the main area of interest from a business perspective. Positioning techniques include Ultra-Wide-Band (UWB) time-(difference-)of-arrival (T(D)oA)-based localisation [1], [2], Angle-of-Arrival (AoA)-based localisation [3], [4], Received Signal Strength (RSS)-based localisation [5], or, when not relying on radio-frequency (RF) signals, using Visible Light Positioning (VLP)-based localisation [6]. For many applications, tracking accuracy requirements are only in the order of metres, making RSS-based localisation systems a popular choice, given their relatively low deployment cost and the compatibility with WiFi- or Bluetooth Low Energy (BLE)-enabled off-the-shelf devices, such as smartphones or tablets. Moreover, these allow the development of localization and navigation Apps showing the user's location and path to the desired destination via a graphical user interface.

Hybrid solutions, combining multiple techniques, are expected to be able to improve localization accuracy. A mathematical approach of hybrid RSS/AoA was recently presented in [7] and applied to a simple box-shaped environment. In [8], two hybrid RSS/ToA localization techniques were presented and compared in a series of simulations. In [9], the principle of AoA estimation using an anchor and a tag, which are built around Decawave's DW1000 impulse radio ultra-wideband IC is described. The advent of such hardware would pave the way for hybrid time-based (e.g., Time-of-Flight (ToF)) and AoA-based approaches. The IEEE 802.11mc standard is expected to be a game changer for localization purposes, as it will enable measuring the WiFi Round-Trip Time (RTT) between access points (APs) and mobile devices, whereas up to now, only RSS measurements have been available. The above efforts indicate the technological trend towards hybrid solutions with the ultimate aim of a higher positioning accuracy. In this paper, a simulation framework for the evaluation of the performance of hybrid indoor localization approaches is presented and applied to a realistic office environment. The simulations are based on experimentally determined accuracies of RSS, AoA, and ToF models. This research will shed light on estimated accuracies that can be achieved when hybrid hardware solutions become available. In Section II, our methodology is presented. Section III presents the results, and the main findings of this paper are summarized in Section IV.

II. Method

The approach of relying on RSS fingerprinting maps for localisation is well known in the research community, see e.g., [5], [10]. These maps can be obtained in two ways. The first is the manual collection of RSS values from all APs at each candidate location, a very time-consuming task. The second way is via model-based fingerprinting, where RSS values at the candidate locations are estimated based on propagation models [11], [5]. By comparing incoming RSS measurements with the expected RSS values, the most likely location is derived, whereby different metrics [12] or probabilistic approaches [13] are possible. In both cases however, the accuracy of the location estimation is largely determined by how much the measured RSS values ('*online*') differ from the fingerprinting map [13] ('*offline*'), or differently stated, from the accuracy of the model that is used to map transmitter (Tx)-receiver (Rx) links to RSS values. This paper is based on the observation that similar fingerprinting maps can be constructed for AoA and/or ToA values. Just like an RSS can be estimated and modeled based on its measurement location relative to the AP, also ToA and AoA models can be incorporated in a positioning framework. This paper will use

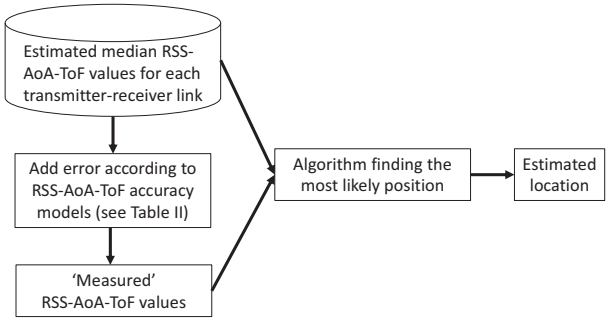

Fig. 1: Flow graph illustrating the procedure of the simulation and the estimation of the position.

experiments from previous research to obtain realistic models and apply them to an office building scenario.

Fig. 1 illustrates the framework for joint RSS-AoA-ToF positioning. First, a database is created with fingerprint values. The RSS value is based on the median path loss that is expected for each of the Tx-Rx links. For AoA and ToF, this fingerprint value is equal to the *real* angle and *real* time-of-flight of each of the Tx-Rx links. Incoming measurements will here be simulated by adding noise to the real AoA and ToF values (lower left box in Fig. 1), or to the expected RSS, as will be described in Sections II-A, II-B, and II-C, respectively. The positioning algorithm is based on the comparison of the incoming measurement with the fingerprint database values, and will be described in Section II-E. Section II-D will present the simulation environment.

A. Angle-of-Arrival

For AoA measurements, WIPP [14] reports a median absolute error of 3°, MaTrack [15] one of about 5° and Cupid [16] one of 20°. These errors are due to multipath and are more severe in Non-Line-of-Sight (NLoS) situations. Therefore, SpotFi [17] reports a different median absolute error for Line-of-Sight (LoS) and NLoS conditions: less than 5° and less than 10° respectively. Fig. 2 shows the empirical cumulative distribution function (cdf) that was obtained in [17] for the SpotFi system, with a differentiation between LoS and NLoS links. We then fitted a model to this empirical cdf. A Laplace distribution showed to better match the empirical cdf than a Gaussian distribution, as was also suggested in [18]:

$$f(x;\lambda) = \frac{1}{2\lambda} exp(-\frac{|x|}{\lambda}), \tag{1}$$

with x the angular error of the measured AoA, and λ a distribution parameter. Fig. 2 shows that Laplace distributions with λ values of 7 and 15 quite accurately represent SpotFi's empirical cdf of [17], for LoS and NLoS situations respectively.

B. Time-of-Flight

The distance d between Tx and Rx is related to the ToF by the speed of light c:

$$d(m) = c(\frac{m}{s}) \cdot ToF(s) \tag{2}$$

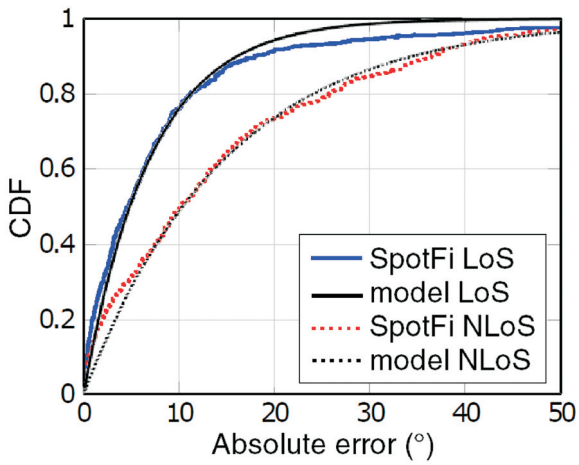

Fig. 2: Comparison of empirical cdf from [17] and Laplace-modeled cdf of absolute Angle-of-Arrival error (λ = 7 for LoS, λ = 15 for NLoS).

The accuracy of ToF measurements was described in [19], where the Chronos system used Channel State Information (CSI) readings from an Intel 5300 Wi-Fi card to estimate the ToF. It appeared that the error was dependent on the distance between Tx and Rx. Similarly like for AoA, also a difference in accuracy was observed between LoS and NLoS situations. Fig. 3 shows the experimentally obtained distance errors (or equivalently, time errors) of the system of [19], with considered distances up to 15 m. We modelled here these median timing errors. Although an *exponential* fit led to slightly higher R^2 values (R^2 = 0.85 (LoS) and 0.92 (NLoS) for exponential vs. 0.81 (LoS) and 0.83 (NLoS) for linear fit), the best *linear* fits will be used for the simulation, since we intend to extrapolate the model to distances larger than 15 m. For these larger distances, the linear fit is expected to be a more truthful representation of reality than the exponential fits. The following formulas for the median (absolute) timing error are obtained for LoS ($|\Delta t|^{LoS}_{err,med}$, eq. (3)) and NLoS ($|\Delta t|^{NLoS}_{err,med}$, eq. (4)) links, respectively.

$$|\Delta t|^{LoS}_{err,med}(ns) = 0.0414(ns/m) \cdot d(m) + 0.2314(ns) \tag{3}$$

$$|\Delta t|^{NLoS}_{err,med}(ns) = 0.088(ns/m) \cdot d(m) + 0.2066(ns) \tag{4}$$

with d (m) the LoS distance between Tx and Rx. To model the standard deviations for each of the distances, we assume that the timing errors Δt originate from a Gaussian distribution. Since the median absolute error (as modeled in eqs. (3) and (4)) can be converted to the standard deviation σ of a Gaussian distribution by multiplying it by 1.4826, we obtain the following formulas for the standard deviations as follows:

$$\sigma_{\Delta t,LoS}(ns) = 0.0614(ns/m) \cdot d(m) + 0.3431(ns) \tag{5}$$

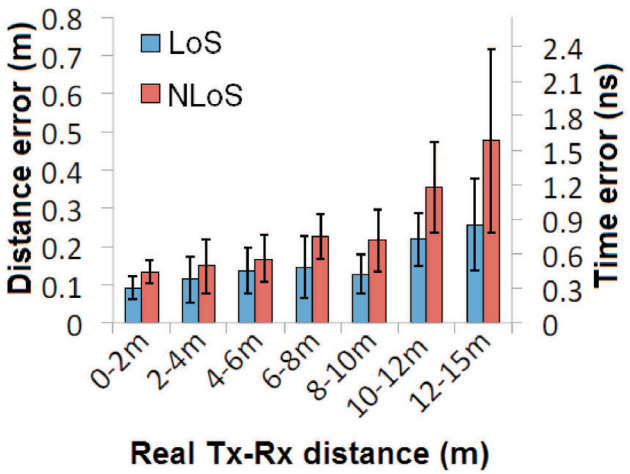

Fig. 3: Empirical (absolute) time and distance errors as reported in [19].

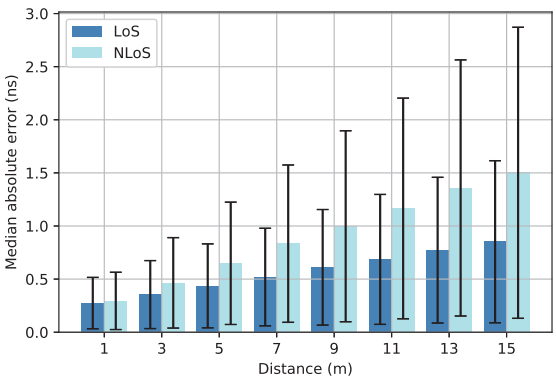

Fig. 4: Modeled (absolute) time errors.

$$\sigma_{\Delta t,NLoS}(ns) = 0.1305(ns/m) \cdot d(m) + 0.3063(ns) \quad (6)$$

It can be observed in Fig. 4 that the modeled timing errors are a reasonably accurate representation of the empirical ones of Fig. 3.

C. RSS

A lot of research has already been dedicated to indoor path loss or RSS modelling. The most commonly followed approach is a one-slope log-distance model, of which the simplest version is the model that uses free-space loss values as estimates. An alternative approach is a two-slope model, e.g., the IEEE 802.11 TGn model [20] for office environments, or more complex models such as, e.g., Indoor Dominant Path Loss models [11]. In all cases, the path loss PL (dB) is estimated as a variation χ (dB) on a median path loss PL_{median} (dB), where PL_{median} depends on the environment (Tx-Rx distance, walls, materials,...). χ represents shadowing effects and is lognormally distributed with zero mean and standard deviation σ_χ (dB), which is an indicator of how well the PL model corresponds to reality [21]:

$$\mathrm{PL} = \mathrm{PL}_{\mathrm{median}} + \chi \quad (7)$$

σ_χ, representing the error on the PL (or RSS) estimation, has typical values (for indoor environments) between 2 and 9 dB. The larger σ_χ, the larger the positioning error will be. In [22], a standard deviation between 3 and 5 dB is reported, depending on the specific measurement conditions. In the following, we will use the TGn path loss model and assume a σ_χ of 5 dB.

D. Simulation configuration

The simulations are executed for an office building floor measuring 27 m by 41 m, consisting of a thick concrete core and plasterboard walls. Different configurations with a varying number of APs (3 to 39) will be considered, as illustrated in Fig. 5.

For the simulations, it is assumed that an AP can measure one or more of the following parameters: RSS, AoA, and/or ToF. (Note: in case no RSS is supported, a more suitable name would be *anchor* instead of *AP*.) Table I defines the seven possible AP types, where a checkmark indicates whether or not an AP supports the corresponding measurement. As such, AP types 4 to 7 allow using more than one positioning-enabling parameter. No mixed configurations are considered, i.e., for a given configuration of Fig. 5, all APs are of the same type (i.e., AP type 1 to 7), resulting in 77 considered setups in total (11 configurations with 7 AP types).

TABLE I: Definition of seven AP types.

AP type	1	2	3	4	5	6	7
RSS	✓	X	X	✓	✓	X	✓
AoA	X	✓	X	✓	X	✓	✓
ToF	X	X	✓	X	✓	✓	✓

For each of these 77 cases, measurements will be simulated 10 times on a rectangular grid with a spacing of 300 cm, with candidate locations each 50 cm. All Txs are considered to have an Equivalent Isotropically Radiated Power of 10 dBm, and the Rxs a sensitivity of -80 dBm. Table II summarizes the statistical distributions of the errors (see Fig. 1) that are used in the simulation scenario.

TABLE II: Statistical AoA, ToF, and RSS error distributions used in the simulation scenario.

Error	**LoS**	**NLoS**
AoA [17] (°)	$\sim$ *Laplace* (0,7)	$\sim$ *Laplace* (0,15)
ToF [19] (ns)	$\sim \mathcal{N}(0, \sigma^2_{\Delta t,LoS})$	$\sim \mathcal{N}(0, \sigma^2_{\Delta t,NLoS})$
RSS [20] (dB)	$\sim \mathcal{N}(0,5^2)$	

E. Positioning algorithm

A cost function C_L is evaluated at each of the candidate locations L, where the location yielding the lowest C_L value, is estimated to be the most likely location:

$$C_L = \sum_{i=1}^{N} 0.495 \cdot \frac{(RSS_{est}^{L,AP_i} - RSS_{meas}^{L,AP_i})^2}{|RSS_{meas}^{L,AP_i}|} + 0.01 \cdot |AoA_{est}^{L,AP_i} - AoA_{meas}^{L,AP_i}| + 0.495 \cdot \frac{(ToF_{est}^{L,AP_i} - ToF_{meas}^{L,AP_i})^2}{|ToF_{meas}^{L,AP_i}|} \quad (8)$$

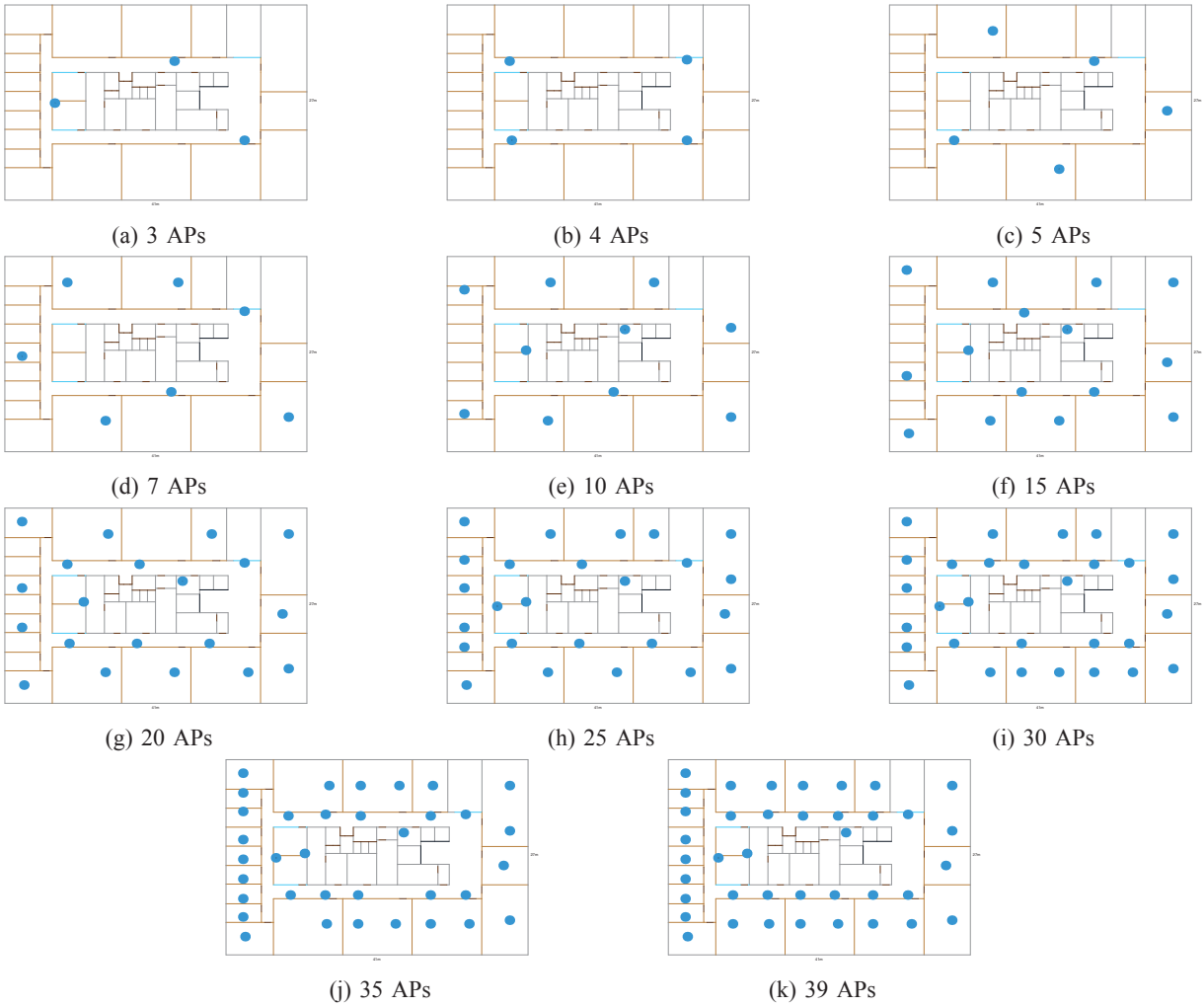

Fig. 5: Floor plan of the simulation environment (27 m x 41 m) for 11 configurations with a different number of APs used (blue dots indicate AP locations).

X_{est}^{L,AP_i} is the value of X, estimated at L and due to AP_i. X_{meas}^{L,AP_i} is a simulated measurement value of X estimated at L and due to AP_i, according to the error models of Table II (X={RSS, AoA, ToF}). N corresponds to the number of installed APs. The metrics (*weighted squared error* for RSS and ToF, and *absolute error* for AoA) were found to perform best in estimating the location, out of 8 possible metrics. The weights 0.495, 0.01, and 0.495 for the respective cost functions were chosen to lead to comparable average cost contributions, but were not optimized towards positioning performance yet.

III. Results

Fig 6 shows the mean positioning error (over the entire building floor grid) for each of the configurations depicted in Fig. 5 and for each of the AP types. For a low number of APs, RSS-only (Type 1) performs better than AoA-only (Type 2), since a low number of APs implies more NLoS Tx-Rx links, for which AoA performs worse. RSS-only accuracy decreases from 5.3 m for 3 APs to around 1.1 m for 39 APs. From around 13 APs on, AoA-only outperforms RSS-only, with errors below 2 m. Using Type 4 APs (hybrid RSS/AoA) further improves the accuracy to below 2 m when using 7 or more APs. APs supporting ToF measurements (Type 3-5-6-7) perform considerably better, with an average error below 1 m already, with as little as 3 APs. Five ToF-enabled APs suffice to achieve a mean accuracy of 53 cm and 10 APs for an accuracy of 33 cm. A minor improvement is obtained when adding AoA to ToF (hybrid AoA/ToF, Type 6), and a minor deterioration when adding RSS to ToF (hybrid RSS/ToF, Type 5). It should be noted that the described performance is valid for the AoA, ToF and RSS models that were presented in Sections II-A,II-B, and II-C. An extensive measurement campaign, covering larger distances ranges in both LoS and NLoS situations, is required to confirm these findings. Alternatively, the *received signal power (RSS)* might be used instead of the *distance*, to model AoA and ToF accuracies. Moreover, depending on the hardware that is used, differences in AoA and ToF estimation accuracy can be expected.

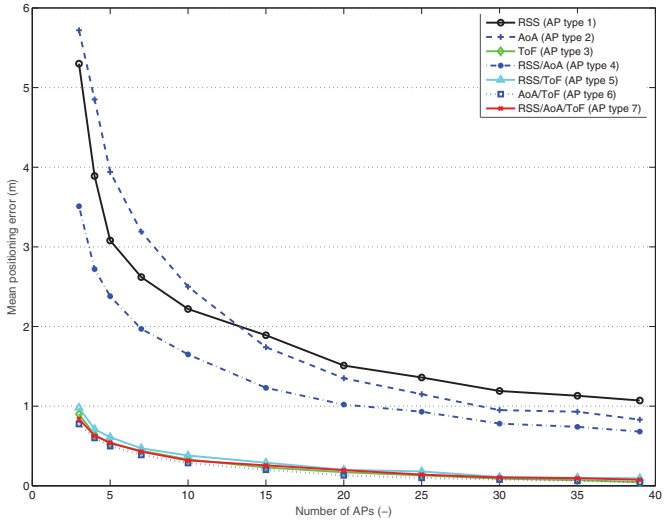

Fig. 6: Positioning error for the different AP types for different numbers of APs on the building floor (see Fig. 5).

IV. Conclusions

In this paper, a software positioning framework is presented. It allows using three different measurement sources: RSS, AoA, and ToF. Based on available empirical data, statistical distributions of measurement accuracies were modeled, in order to truthfully represent a realistic scenario. For the considered hardware (Chronos [19] for ToF and SpotFi [17] for AoA), ToF is the most accurate parameter for positioning, with errors below 1 m for only 3 APs. RSS and AoA have a similar performance, with errors around 2 m for 13 deployed APs. Hybrid RSS/AoA achieves this error with only 7 APs. Future work includes the simulation of other metrics for estimating the most likely position and an optimization of the global cost function. Also AP configurations combining different AP types will be investigated (e.g., two ToF-only APs with 5 RSS-only APs). A main future research topic is the construction of a more complete accuracy model in LoS and NLoS for different distances with real hardware, and a subsequent experimental validation of the framework.

References

[1] D. Dardari, A. Conti, U. Ferner, A. Giorgetti, and M. Z. Win, "Ranging with ultrawide bandwidth signals in multipath environments," *Proceedings of the IEEE*, vol. 97, no. 2, pp. 404–426, 2009.

[2] N. Podevijn, D. Plets, J. Trogh, L. Martens, P. Suanet, K. Hendrikse, and W. Joseph, "TDoA-based Outdoor Positioning with Tracking Algorithm in a Public LoRa Network," *Wireless Communications and Mobile Computing*, in press.

[3] E. Elnahrawy, J. Austen-Francisco, and R. P. Martin, "Adding angle of arrival modality to basic rss location management techniques," in *Wireless Pervasive Computing, 2007. ISWPC 07. 2nd International Symposium on. IEEE*, 2007.

[4] N. BniLam, G. Ergeerts, D. Subotic, J. Steckel, and M. Weyn, "Adaptive probabilistic model using angle of arrival estimation for iot indoor localization," in *2017 International Conference on Indoor Positioning and Indoor Navigation (IPIN)*, Sept 2017, pp. 1–7.

[5] J. Trogh, D. Plets, L. Martens, and W. Joseph, "Advanced real-time indoor tracking based on the viterbi algorithm and semantic data," *International Journal of Distributed Sensor Networks*, vol. 11, no. 10, 2015. [Online]. Available: http://dsn.sagepub.com/content/11/10/271818.abstract

[6] W. Raes, D. Plets, L. D. Strycker, and N. Stevens, "Experimental evaluation of the precision of received signal strength based visible light positioning," in *2018 11th International Symposium on Communication Systems, Networks Digital Signal Processing (CSNDSP)*, July 2018, pp. 1–4.

[7] S. Tomic, M. Beko, R. Dinis, and L. Bernardo, *Sensors (Basel)*, vol. 18, no. 4, April 2018.

[8] T. Panichcharoenrat and W. Lee, "Two hybrid rss/toa localization techniques in cognitive radio system," in *2014 6th International Conference on Knowledge and Smart Technology (KST)*, Jan 2014, pp. 23–28.

[9] I. Dotlic, A. Connell, H. Ma, J. Clancy, and M. McLaughlin, "Angle of arrival estimation using decawave dw1000 integrated circuits," in *2017 14th Workshop on Positioning, Navigation and Communications (WPNC)*, Oct 2017, pp. 1–6.

[10] Y. Wen, X. Tian, X. Wang, and S. Lu, "Fundamental limits of rss fingerprinting based indoor localization," in *2015 IEEE Conference on Computer Communications (INFOCOM)*, April 2015, pp. 2479–2487.

[11] D. Plets, W. Joseph, K. Vanhecke, E. Tanghe, and L. Martens, "Simple indoor path loss prediction algorithm and validation in living lab setting," *Wireless Personal Communications*, pp. 1–18, 10.1007/s11277-011-0467-4. [Online]. Available: http://dx.doi.org/10.1007/s11277-011-0467-4

[12] D. Plets, A. Eryildirim, S. Bastiaens, N. Stevens, L. Martens, and W. Joseph, "A performance comparison of different cost functions for rss-based visible light positioning under the presence of reflections," in *Proceedings of the 4th ACM Workshop on Visible Light Communication Systems at the 23rd Annual International Conference on Mobile Computing and Networking*. ACM Press, 2017, pp. 37–41. [Online]. Available: http://dx.doi.org/10.1145/3129881.3129888

[13] R. Guan and R. Harle, "Signal fingerprint anomaly detection for probabilistic indoor positioning," in *2018 International Conference on Indoor Positioning and Indoor Navigation (IPIN)*, 2018.

[14] Z. Zhang, Z. Tian, M. Zhou, Z. Li, Z. Wu, Y. Jin, and C. V. Verikoukis, "Wipp: Wi-fi compass for indoor passive positioning with decimeter accuracy," 2016.

[15] X. Li, S. Li, D. Zhang, J. Xiong, Y. Wang, and H. Mei, "Dynamic-music: accurate device-free indoor localization," 09 2016, pp. 196–207.

[16] S. Sen, J. Lee, K.-H. Kim, and P. Congdon, "Avoiding multipath to revive inbuilding wifi localization," in *MobiSys*, 2013.

[17] M. Kotaru, K. Joshi, D. Bharadia, and S. Katti, "Spotfi: Decimeter level localization using wifi," *SIGCOMM Comput. Commun. Rev.*, vol. 45, no. 4, pp. 269–282, Aug. 2015. [Online]. Available: http://doi.acm.org/10.1145/2829988.2787487

[18] R. Peng and M. L. Sichitiu, "Angle of arrival localization for wireless sensor networks," in *2006 3rd Annual IEEE Communications Society on Sensor and Ad Hoc Communications and Networks*, vol. 1, Sept 2006, pp. 374–382.

[19] D. Vasisht, S. Kumar, and D. Katabi, "Sub-nanosecond time of flight on commercial wi-fi cards," *CoRR*, vol. abs/1505.03446, 2015. [Online]. Available: http://arxiv.org/abs/1505.03446

[20] Q. Li, M. Ho, V. Erceg, A. Jangantham, and N. Tal, "802.11n channel model validation," IEEE 802.11-03/894r1, 11-03-0894-01-000n-802-11n-channel-model-validation.pdf," Tech. Rep., 2003.

[21] J. Trogh, D. Plets, A. Thielens, L. Martens, and W. Joseph, "Enhanced indoor location tracking through body shadowing compensation," *IEEE Sensors Journal*, vol. 16, no. 7, pp. 2105–2114, April 2016.

[22] Y. Chapre, P. Mohapatra, S. Jha, and A. Seneviratne, "Received signal strength indicator and its analysis in a typical wlan system (short paper)," in *38th Annual IEEE Conference on Local Computer Networks*, Oct 2013, pp. 304–307.